

Curious Morphology of Silicon-Containing Polymer Films on Exposure to Oxygen Plasma

Vanessa Z.-H. Chan and Edwin L. Thomas

Department of Materials Science and Engineering, Massachusetts Institute of Technology, 77 Massachusetts Avenue, Cambridge, Massachusetts 02139

Jane Frommer,* David Sampson, Richard Campbell, Dolores Miller, Craig Hawker, Victor Lee, and Robert D. Miller

IBM Almaden Research Center, 650 Harry Road, San Jose, California 95120

Received April 30, 1998. Revised Manuscript Received August 12, 1998

Thin films of silicon-containing polymers were studied to investigate changes in surface composition and morphology on exposure to an oxygen plasma. For low molecular weight poly(pentamethyldisilylstyrene) (P(PMDSS)), a reticulated structure was observed by atomic force microscopy (AFM) that could limit future lithographic applications of these materials. The reticulations were of approximately 1 μm in width and 5 μm in length, though a higher molecular weight polymer resulted in smaller feature sizes. In polysilane polymers containing silicon in the backbone and molecular weights significantly larger than the entanglement molecular weight, the feature dimensions were even smaller. Films etched at lower temperature (0 °C) displayed none of the reticulated morphology, retaining instead the smooth appearance of pre-etched films. It was found by X-ray photoelectron spectroscopy (XPS) and Auger electron spectroscopy (AES) that a thin (<100 Å) layer of SiO_x formed on the surface of all of the studied silicon-containing polymer films. Appearance of the reticulated morphology required the combined presence of heating, oxygen plasma, and silicon in the polymer. The reticulated structures are believed to result from the destabilization of the thin films as they undergo the transition from a nonpolar organosilane to a polar oxide.

I. Introduction

In the past 10 years there has been extensive research on the development of new polymers for microlithographic patterning. One focus of this research, particularly for bilayer applications, has been on silicon-containing polymers that form a protective oxide layer when exposed to an oxygen plasma.^{1,2} The etch resistance of this oxide to the oxygen plasma provides the selectivity needed for lithographic image transfer. For this reason, considerable effort has been devoted to understanding the mechanism behind the formation of this protective oxide coating.

Various silicon-containing polymers have been investigated, including silicon-substituted novolacs, methacrylates, olefinsulfones, and styrenes as well as polysilanes, silylated organic resists, and siloxane copolymers.¹ These studies have focused mainly on the lithographic properties, such as imaging, pattern transfer, and etch selectivity. Characterization techniques have included Auger electron spectroscopy (AES), X-ray photoelectron spectroscopy (XPS), Rutherford backscattering (RBS), and scanning electron microscopy (SEM). Relatively little work has utilized atomic force microscopy (AFM) as a technique for studying the evolution of surface morphologies upon etching.³

Chou et al. investigated the elemental composition of surfaces of plasma-etched silicon-containing polymers by AES and XPS and found that a 10 Å thick oxide layer persists throughout the reactive ion etch (RIE) process.⁴ This steady-state layer formation results from the competing processes of oxide growth vs ion sputtering from the surface. These authors also found that although the oxide is physically removed by ion sputtering, it is not chemically etched by the oxygen plasma. It is this characteristic that produces the important etch selectivity for silicon-containing polymers versus those without silicon.

Gokan et al. studied organosilicon polymers and found that the etch resistance increased with increasing silicon content in the polymer. They found that if a minimum of 1×10^{16} Si atoms/cm² were present on the polymer surface, etching ceased after the formation of the oxide layer.⁵ Similarly, other researchers^{6,7} have found that the O₂-RIE resistance rapidly improves with increasing

(3) Petri, R.; Brault, P.; Vatel, O.; Henry, D.; Andre, E.; Dumas, P.; Salvan, F. *J. Appl. Phys.* **1994**, *75* (11), 7498–7506.

(4) Chou, N. J.; Tang, C. H.; Paraszczak, J.; Babich, E. *Appl. Phys. Lett.* **1985**, *46*, 31–33.

(5) Gokan, H.; Saotome, Y.; Saigo, K.; Watanabe, F.; Ohnishi, Y. In *Polymers for High Technology, Electronics, and Photonics*, Anaheim, CA; Turner, S. R., Bowden, M. J., Eds.; ACS Symposium Series; American Chemical Society: Washington, D.C., 1986; pp 358–368.

(6) Ohnishi, Y.; Suzuki, M.; Saigo, K.; Saotome, Y.; Gokan, H. *Advances in Resist Technology and Processing II*; SPIE Vol. 539; SPIE: Bellingham, WA, 1985; p 62–69.

(7) Reichmanis, E.; Smolinsky, G. *Advances in Resist Technology and Processing*; SPIE Vol. 469; SPIE: Bellingham, WA, 1984; p 38–43.

(1) Miller, R. D.; Wallraff, G. M. *Adv. Mater. Opt. Electron.* **1994**, *4*, 95–127.

(2) Hartney, M.; Hess, D.; Soane, D. J. *Vac. Sci. Technol. B* **1989**, *7*, 1–13.

silicon content, leveling off at a critical concentration of approximately 10–15 wt % silicon.

Models have been developed for the growth of this oxide layer in an oxygen plasma where the growth rate follows a steady-state process.⁸ In these models, the growth rate was diffusion-limited, inversely proportional to oxide thickness, and limited to a maximum oxide thickness, after which further growth of the oxide layer ceased. Other researchers have expanded this steady-state model^{9,10} and found that there were at least two regimes for oxide formation. In regime I, the transition regime, the etch rate is positive, since the carbon moieties in the polymer are removed before a contiguous protective SiO_x barrier is formed. Regime II, the steady-state regime, follows, where an effective SiO_x barrier has been formed and the etch rate becomes essentially constant; i.e., the rate of oxide removal by ion sputtering equals the rate of oxide growth.

In their study of oxide growth mechanisms, researchers have also examined the effects of substrate temperature on the etching of silicon and silicon-containing resists. Durandet et al. have shown in certain cases, due to ion bombardment, the silicon wafer can reach temperatures of above 200 °C if there is not near-perfect thermal contact between the substrate and substrate holder since only radiative losses are possible.¹¹ In non-silicon-containing novolac resins, Joubert et al. explored resist degradation in both oxygen and argon plasmas and showed that substrate cooling prevents degradation of the resist throughout the bulk by preventing self-diffusion of polymer chains which otherwise would renew the surface with fresh chains. However, it should be noted that the molecular weights of the polymers used in this study were low (1000–2000 g/mol), leading to accelerated diffusion.¹² Joubert et al. have also investigated O₂-RIE processes in silicon-containing resists and found that an increase in the substrate temperature to ~100 °C results in a liquefaction of the top surface silylated areas. This resulted in redistribution of the silicon throughout the bulk resist due to diffusion of the silylated chains, thereby preventing the formation of a contiguous solid mask.¹³ Various investigators have also found that wafer temperature strongly influences the etch rate of silicon-containing resists; e.g., cooling the substrate results in a higher etch rate.^{11,14,15} This was attributed to either the decrease in reactivity between Si and reactive oxygen species or the decrease in the mobility of the Si during RIE. It has also been

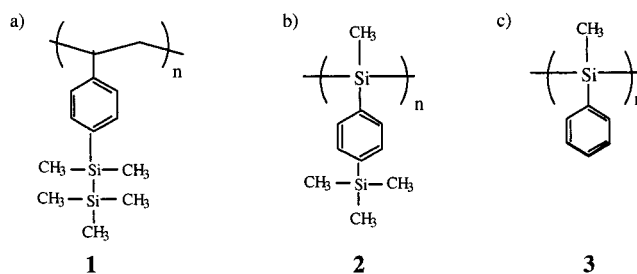


Figure 1. Chemical structures of silicon-containing polymers synthesized for this study: poly(pentamethyldisilylstyrene) (1), poly((4-(trimethylsilyl)phenyl)methylsilane) (2), and poly(phenylmethylsilane) (3).

shown in low- T_g novolacs that, with higher substrate temperature, the etch rate increases in a steplike manner due to higher mobility of the polymer system.^{16,17} However, it should be noted that all these experiments were performed on relatively thick (0.5–1 μm) silylated resist layers. With thin (<0.5 μm) films the opposite effect is noted: cooling reduces the amount of material removed before an effective oxide barrier layer is formed.¹¹

Here we report the formation of an unusual reticulated surface morphology observed by AFM in three silicon-containing polymers on exposure to an oxygen plasma at ambient plasma temperatures. The percent silicon in these polymers varies from 23 to 29% with the silicon situated in either the backbone or in a pendant group, or both, as seen in Figure 1. Surface roughening of organosilicon polymers has been reported by others.^{11,13,15} However, no extensive AFM studies have been reported with structures similar to the ones here, perhaps due to differences in polymer structures, reactive ion etch tools, and etch parameters such as gas pressure, oxygen flow rate, etching times, magnetic enhancement, and RF power.

Our observations are relevant for the high-resolution etching of photoresists where side wall and edge uniformity are important for accurate pattern transfer. To meet the demanding lithographic requirements for future devices with very small features, it is necessary to minimize sources of surface and pattern roughening in pattern-transfer lithography.

II. Experimental Procedures

A. Polymer Synthesis. The principal polymer employed in this study is a homopolymer of pentamethyldisilylstyrene (PMDSS)¹⁸ synthesized by "living" free radical polymerization, **1a**. The polymer structure is shown in Figure 1, and its properties are tabulated in Table 1. The polymer was prepared by free radical initiation in the presence of nitroxides.¹⁹ The polymerization was performed at 125 °C without solvent under an argon atmosphere for approximately 24 h. The polymer was then precipitated in methanol and was not further fractionated.

(16) Joubert, O.; Paniez, P.; Pelletier, J.; Pons, M. *Appl. Phys. Lett.* **1991**, *58* (9), 959–961.

(17) Paniez, P. J.; Joubert, O. P.; Pons, M. J.; Oberlin, J.-C.; Weill, A. P. *Advances in Resist Technology and Processing*, SPIE Vol. 1466; SPIE: 1991; pp 583–591.

(18) The monomer was synthesized following a modified literature procedure (Kawakami, Y.; Hisada, H.; Yamashita, U. *J. Polym. Sci., Polym. Chem.* **1988**, *26*, 1307).

(19) Hawker, C. J.; Elce, E.; Dao, J.; Volksen, W.; Russell, T. P.; Barclay, G. *Macromolecules* **1996**, *29*, 2686–2688.

(8) Watanabe, F.; Ohnishi, Y. *J. Vac. Sci. Technol. B* **1986**, *4*, 422–425.

(9) Jurgensen, C. W.; Shugard, A.; Dudash, N.; Reichmanis, E.; Vasile, M. J. *SPIE, Advances in Resist Technology and Processing V*; SPIE Vol. 920; SPIE: Bellingham, WA, **1988**; pp 253–259.

(10) Dijkstra, J. *Advances in Resist Technology and Processing*; SPIE Vol. 1466; SPIE: Bellingham, WA, 1991; pp 592–603.

(11) Durandet, A.; Joubert, O.; Pelletier, J.; Pichot, M. *J. Appl. Phys.* **1990**, *67* (8), 3862–3868.

(12) Joubert, O.; Fiori, C.; Oberlin, J. C.; Paniez, P.; Pelletier, J.; Pons, M.; Vachette, T.; Weill, A. *J. Appl. Phys.* **1991**, *69* (3), 1697–1702.

(13) Joubert, O.; Claude, R.; Pons, M.; Weill, A.; Paniez, P. *Advances in Resist Technology and Processing IX*; SPIE Vol. 1672; SPIE: Bellingham, WA, 1992; pp 561–572.

(14) Gokan, H.; Saotome, Y.; Saigo, K.; Watanabe, F.; Ohnishi, Y. In *Polymers for High Technology, Electronics, and Photonics*, Anaheim, CA; Turner, S. R., Bowden, M. J. Eds.; ACS Symposium Series; American Chemical Society: Washington, D.C., **1987**; pp 358–368.

(15) Bobbio, S. M.; Jones, S. K.; Tessier, T. G.; Dudley, B. W.; Cohen, B.; Russell, F. J.; Morosoff, A. *SPIE* **1989**, *1185*, 24–33.

Table 1. Characterization of Silicon-Containing Polymers Used in This Study: Molecular Weight, Polydispersity, Glass Transition Temperature (T_g), % Si and RMS Roughness after O_2 -RIE for 60 s at Plasma Temperature

sample	M_n	M_w/M_n	T_g , °C	% Si	RMS roughness, nm
poly(pentamethyldisilylstyrene) (PMDSS)					
anionic (1b)	34 000	1.06	107	24	24
living free radical (1a)	10 800	1.83	80	24	37
poly((4-(trimethylsilyl)phenyl)methylsilane) (2)	223 100	2.6	120	29	17
poly(phenylmethylsilane) (3)	262 200	3.2	117	23	5

Poly(PMDSS)²⁰ (P(PMDSS) was also prepared by anionic polymerization, **1b**, and the resulting material compared to that prepared by living free radical techniques. The ¹H NMR, ¹³C NMR, ²⁹Si NMR, and FTIR spectra of the free radical and anionically prepared P(PMDSS) samples were identical and are available as Supplemental Information. The polydispersity was lower and the molecular weight higher for material produced by anionic polymerization. The elemental analysis of **1b** was consistent with the proposed structure.²¹

For comparison, two other silicon-containing polymers with very different structures were also investigated, and their polymer properties are reported in Table 1. Poly((4-(trimethylsilyl)phenyl)methylsilane) **2**, and poly(phenylmethylsilane) **3**, were both prepared via Wurtz-coupling polymerization.²² Their chemical structures are also shown in Figure 1.

It should be noted that the weight percentages of silicon in all of the polymers studied were greater than 10%, the critical value needed to form an effective oxide barrier during reactive ion etching in an oxygen plasma.^{6–8}

B. Sample Preparation. Solutions of P(PMDSS) **1a,b** were prepared in toluene (5 wt %). The other two silane polymer solutions, **2** and **3**, were adjusted to lower concentrations in xylene (1.5–3 wt %) due to the much higher molecular weights of these samples. Polymer films were made by spin-coating onto 1 in. (100) silicon wafers with a native oxide. The silicon substrates were cleaned with toluene prior to spinning, and the polymer solution was deposited onto the Si wafers using a syringe tipped with a 0.45 μ m filter. Films were prepared by spinning first at 500 rpm for 15 s and then at 1500 rpm for 40 s. All film samples were baked in a vacuum oven at 70 °C for at least 12 h to remove residual solvent. Final film thicknesses were measured with a mechanical profilometer and found to range between 200 and 300 nm.

C. Plasma Etching. The etching experiments were carried out in a low-pressure, magnetically enhanced, inductively coupled, plasma etcher. Etching was performed with a base pressure of 10 mTorr and an oxygen flow rate of 40 cm³(STP) min⁻¹. The top radio frequency (rf) generator was set at 250 W, and the bottom rf generator, at 50 W. Etching was performed at either ambient plasma temperature or 0 °C. It was estimated that the *minimum* sample temperature was 70 °C in the ambient plasma; the actual temperature could be much higher.²³ The wafer temperature was estimated by placing liquid crystal temperature dots on a silicon wafer, covering them with Kapton tape to protect the chamber from etching products, and exposing them to the same etching conditions as used for the polymers for 60 s. Polymer etching times were 10 s, 20 s, 30 s, 60 s, or 5 min.

For samples etched at 0 °C, the backside of the wafer was first coated with In–Ga in order to improve the thermal contact of the samples to the cold chuck. The sample chuck sits above a reservoir of liquid nitrogen above which a stream of helium passes which conducts heat away from the wafer backside. The temperature of the system is regulated by a thermocouple sitting on the sample chuck which is equipped with a feedback loop to a resistive heater. The wafers were backside cooled by the helium gas, and the temperature was

allowed to equilibrate for 15 min before etching. During etching, the actual surface temperature of the sample may be higher than the measured temperature at the chuck since the surface is heated due to ion bombardment. However, since the polymer samples are thin films and the silicon substrate is a relatively good heat conductor, the temperature difference between the chuck and the sample should be minimal.

D. Atomic Force Microscopy. The atomic force microscopy images were collected with a commercial instrument employing optical deflection detection. Standard silicon cantilevers were used for intermittent contact imaging mode. Data were acquired on frames ranging from 250 nm \times 250 nm to 50 μ m \times 50 μ m having 256 \times 256 data points. Images were recorded using both height and phase-shift channels. AFM measurements yielded surface feature dimensions and the root mean square (RMS) surface roughness.²⁴ RMS results were compared between images of equal scan size (50 μ m \times 50 μ m) to minimize scan size dependencies.

E. Auger Electron Spectroscopy. A commercially available scanning Auger microprobe was used. The electron energy was 10 keV, and the electron current was 1 A. Sample sputtering for depth profiling was accomplished with a 3 keV argon ion beam over a 2 \times 2 mm² raster.

F. X-ray Photoelectron Spectroscopy. The atomic concentrations of silicon, carbon, and oxygen were estimated by X-ray photoelectron spectroscopy. Analysis was done on an ESCA spectrometer with a monochromatic Al K α source. Survey spectra at 1000 eV were recorded at 150 eV pass energy with a 1000 μ m spot size for each sample. High-resolution spectra (50 eV pass energy, 20–30 eV window) were recorded for carbon, oxygen, and silicon.

Variable angle XPS studies of the samples were conducted in order to estimate possible surface contamination. Data were taken at two detector-to-sample angles: 10 and 60°. The 10° data provide information on approximately the top 15 Å of the film, while the 60° data sample the top 75 Å, assuming a mean free path of about 25 Å for the \sim 1400 eV kinetic energy Si 2p photoelectrons through the polymer film. This estimate also assumes a flat sample surface.

G. Contact Angle Measurements. The surface energies of the P(PMDSS) samples both before and after plasma etching for 60 s at 0 °C were determined by contact angle measurements using hexadecane or water. Using the Girifalco–Godd–Fowkes–Young equation, the corresponding surface energies were calculated.²⁵

III. Results

All of the as-deposited polymers studied were determined by AFM to be smooth before etching, with a RMS roughness of \sim 0.7 nm. As a control for the profilometry and AFM experiments, a 700 Å thick polystyrene (PS) film was spun onto a silicon wafer and etched under the same ambient plasma conditions as the silicon-containing polymers. After short etching times (<60 s) AFM indicated there was no roughening of the surface. After 60 s, the PS film was removed entirely, corresponding to an etch rate of at least 700 Å/min.

(20) Avgeropoulos, A.; Chan, V. Z. H.; Lee, V.; Ngo, D.; Miller, R. D.; Hadjichristidis, N.; Thomas, E. L. *Chem. Mater.* **1998**, *10*, 2109–2115.

(21) Supplemental information on the structure analysis of the polymers is available on request.

(22) Miller, R. D.; Michl, J. *Chem. Rev.* **1989**, *89*, 1359–1410.

(23) Deleted in proof.

(24) *Command Reference Manual*, Version 4.10.01; Digital Instruments: Santa Barbara, CA 1996; p 12.67.

(25) Fowkes, F. M. *Chemistry and Physics of Interfaces*; American Chemical Society: Washington, D.C., 1965; pp 1–12.

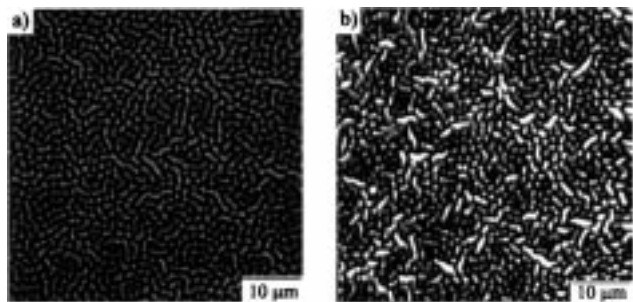


Figure 2. Topography of **1a** P(PMDSS) after exposure to O₂-RIE for (a) 20 and (b) 60 s.

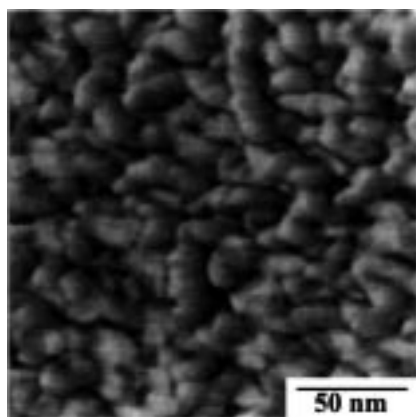


Figure 3. Substructure on reticulations in Figure 2a. z-scale = 10 nm.

Table 2. RMS Roughness (nm) of P(PMDSS) (**1a**) for Different Etch Times

etch time, s	RMS roughness, nm
0	0.7
10	15
30	26
60	37

As a control experiment for determining the effect of heating alone on the polymers, samples of as-deposited P(PMDSS) **1a** were heated to 120 °C for 1 h in either nitrogen or air. No significant surface roughening was observed by AFM: the RMS of both unetched films and unetched heated films was less than 1 nm.²⁶

Figure 2 shows the evolution of morphology with etch time in the lower molecular weight P(PMDSS) sample, **1a**. At short etch times (Figure 2a), the origin of the reticulated surface morphology is more obviously seen as an alignment of neighboring hemispherical structures that grow in height with an increase in etch time (Figure 2b). This vertical growth is manifested as an increase in RMS roughness with etch time (Table 2). As seen from Figure 3, a substructure *within* the reticulated morphology is composed of particles 0.05–0.25 μm in diameter.

The higher molecular weight P(PMDSS), **1b**, also develops a morphology after etching for 60 s at ambient plasma temperature (Figure 4a). However, instead of the formation of elongated structures as in the case for **1a**, this sample produces only small spherical features

of approximately 0.5 μm diameter. The RMS roughness is similar to that of the earlier stages of etched **1a**, when the small hemispherical structures were most prominent (Table 2). This difference in morphology between **1a** and **1b** could be attributed to differences in sample molecular weight. The molecular weight of **1b** is three times that of **1a**, and hence the polymer chains are expected to be less mobile during reactive ion etching. The polydispersity is lower for **1b**, another possible contributing factor to the size difference in the surface morphology.

The molecular weights of both P(PMDSS) samples are probably below their entanglement molecular weights. The entanglement molecular weight for P(PMDSS) **1** is crudely estimated to be ~68 000 simply on the basis of the ratio of the molecular weights of the PMDSS monomer and styrene monomer.²⁷ Since the molecular weights of **1a,b** are both lower than the estimated entanglement molecular weight, alternative silicon-containing polymers with higher molecular weights (Table 1) were also studied. Poly(4-(trimethylsilyl)phenyl)methylsilane **2** and poly(phenylmethylsilane) **3** were etched at ambient plasma temperature for 60 s. As seen from Figure 4b,c, the striking reticulated morphology is not immediately apparent to the eye. However, as seen from the higher magnification inserts of 1 μm scans, the reticulated morphology *does* develop in these samples, albeit at smaller dimensions than in polymer **1**: ~0.4 μm in diameter and 1 μm in length for polymers **2** and **3** compared to ~1 μm in diameter and 5 μm in length for P(PMDSS) (**1a**).

The smaller feature size for polymers **2** and **3** may be caused by their higher initial molecular weights—lower chain mobility would prevent the full development of the reticulated morphology. Another factor to consider is silicon content and environment. The silicon content of polymers **2** and **3** is higher than in **1a** and **1b**, and the silicon is present in the polymer backbone. These two factors would result in more rapid conversion to SiO_x during O₂-RIE. Finally, cross-linking reactions in aryl substituted polysilanes **2** and **3** could lower chain mobilities. The cross-linking of such polymers upon irradiation has been reported elsewhere.²¹

Since it is believed that the mobility of the polymer and its oxidized species may influence morphology, **1a** and **1b** were cooled to 0 °C during etching, well below the *T_g* of the native polymer. The intention was to determine the effect of etching temperature on the resulting surface morphology. AFM images revealed no reticulated features in the final films; the surfaces were comparable to the unetched films with a RMS of 0.7 nm. The absence of a notable surface topography in the samples etched at 0 °C indicates that the formation of surface morphology is a thermally driven process. Ongoing experiments on subsequent heating of these cold-etched films support the differentiation between oxidation and mobilization processes.

The chemical composition of both P(PMDSS) **1a** and **1b** samples before and after etching was found to be

(26) Very thin films (ca. 20 nm) do exhibit a slow evolution of surface structure on standing at room temperature (studies ongoing in our laboratories).

(27) The molecular weights of PMDSS and styrene are 234 and 104, respectively. However, over half of the PMDSS molecular weight results from the silicon-containing side group, so its contribution to entanglement is minimal. As an approximation of entanglement molecular weight, it was assumed that the same number of monomer units are needed to entangle P(PMDSS) as PS.

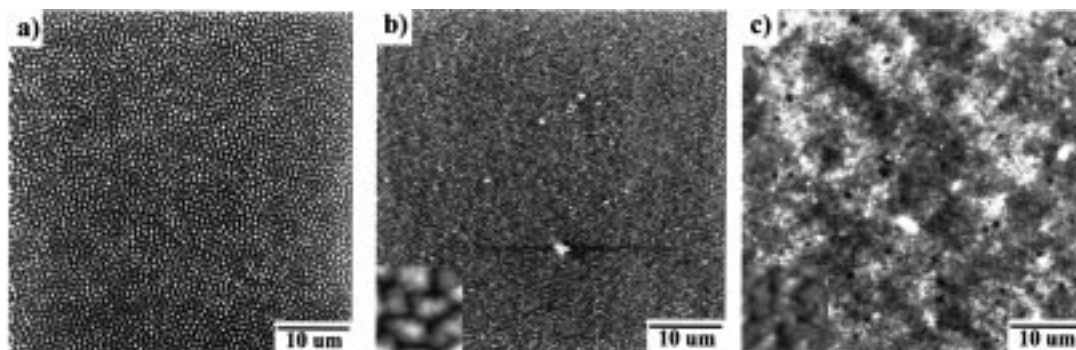


Figure 4. Topography of silicon-containing polymers on etching: (a) **1b**, P(PMDSS), higher molecular weight; (b) **2**, poly(4-(trimethylsilyl)phenyl)methylsilane; (c) **3**, poly(phenylmethylsilane). Insets are $1 \mu\text{m} \times 1 \mu\text{m}$.

Table 3. Binding Energy (eV) and Atomic Concentration (%) of Films before and after Exposure to RIE^a

film	take-off angle	C-bound Si	SiO	SiO ₂	C	O
P(PMDSS) native	60	100.5 (9.3%)	101.5 (6.3%)	NA	284.6 (77.1%)	532.3 (7.4%)
	10	100.4 (4.8%)	102.3 (15%)		284.6 (61.7%)	532.2 (18.5%)
P(PMDSS) etched at 0 °C for 60 s	60	NA	NA	103.5 (24.4%)	284.6 (19.1%)	532.6 (56.5%)
	10			103.2 (24.4%)	284.6 (16.1%)	532.6 (59.6%)
binding energy lit. values ³²		100–101	101.5	103.7		

^a NA = not applicable.

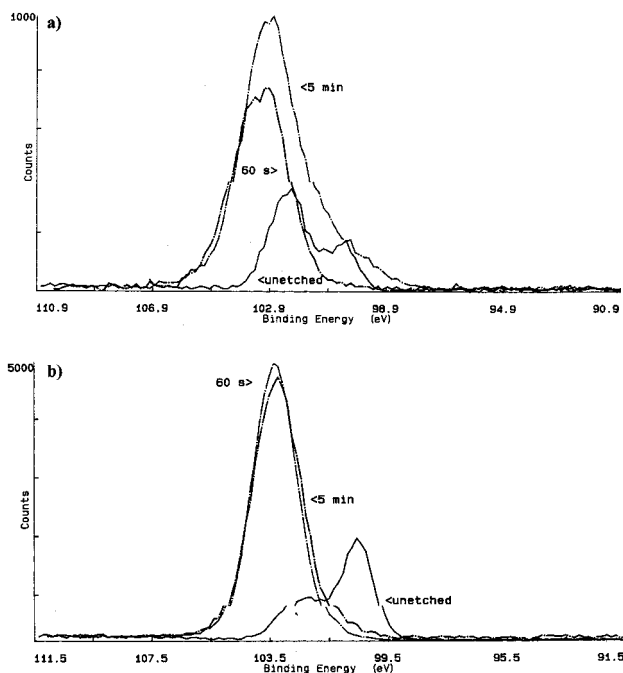


Figure 5. X-ray photoelectron spectroscopy data of **1a** P(PMDSS) before and after oxygen reactive ion etching at 0 °C. Data taken at sample-to-detector angle of (a) 10 and (b) 60°.

identical by XPS. The binding energy of the Si 2p peak was monitored closely as it reflects the chemical environment of the silicon (Table 3, Figure 5). In the unetched samples, the silicon exists mainly in a carbon-rich environment, as seen by the atomic concentration of silicon species with a binding energy peak centered at 100 eV. There is some oxidation of the surface of the as-cast polymer film, as evidenced by the peak at ~102 eV. The ratio of this peak to the silicon in a carbon matrix peak at ~100 eV is much larger at the 10° takeoff angle (~15 Å detection depth) than at the 60° angle (~75 Å detection depth), indicating that the oxidation is concentrated at the topmost surface (see Experimental Procedures). Once the films are exposed

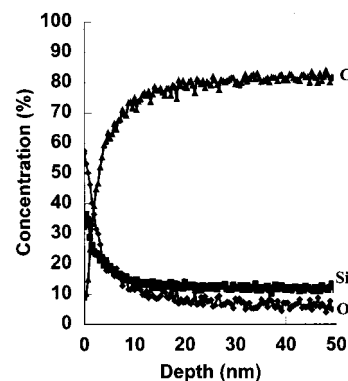


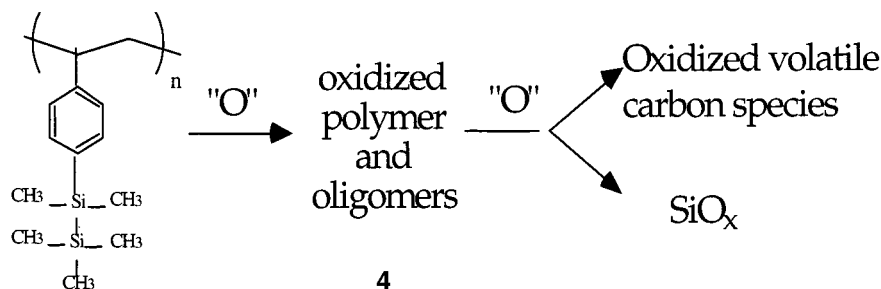
Figure 6. Auger electron spectroscopy of P(PMDSS) after oxygen reactive ion etching at 0 °C.

to an oxygen plasma, the amount of carbon detected by XPS decreases significantly. The most obvious change in the silicon XPS spectrum on etching is the shift in the Si 2p binding energy from 100.5/101.8 to 103.5 eV, indicating that the silicon near the surface of the film has been converted to SiO_x (Table 3). When the data for the etched sample are modeled as a thin surface layer of SiO_x on top of an underlying carbon-rich film (i.e. all detected oxygen is silicon-bound, not carbon-bound), a ratio of O/Si of 1.8 is calculated at the outer surface for the etched samples.

The AES data obtained for **1b** etched for 60 s at 0 °C are consistent with the XPS results. Depth profiling (argon ion sputtering) reveals that the oxygen-to-silicon ratio decreases from its highest value for SiO₂ at the surface to nearly zero for the unetched polymer **1** (Figure 6).

The surface free energies as calculated from contact angle measurements²⁶ on P(PMDSS) before and after reactive ion etching (60 s, 0 °C) were 42.0 and 70.8 erg/cm², respectively. These energies corroborate the XPS and AES data: the higher surface free energy of the RIE-treated sample is consistent with an increase in surface polarity upon conversion of the silicon in the polymer to silicon oxide. For comparison, literature

Scheme 1



values for the surface free energy of polystyrene and silica²⁸ are 34 and 78 erg/cm², respectively.

IV. Discussion

We discuss the reaction of the silicon-containing polymers during RIE in terms of chemical reaction pathways and interfacial material phenomena, as seen from Scheme 1.

In the initial step, the native silicon-containing polymer reacts with the oxygen plasma to form a complex mixture of oxidized oligomers and polymers, designated generically as **4** (Scheme 1). In addition to collision-induced bond cleavage, initial reaction products result from oxygen radical and ion attack, forming various C–O and Si–O species. Hence **4** can be initially described as composed of more polar oxygenated species that lie atop unreacted nonpolar starting material. Silanols and siloxanes, for example, have been observed as reaction products of silanes exposed to RIE conditions. Carbon substituents produce intermediates such as alcohols, aldehydes, ketones, and acids.²¹ The newly created polar species are likely to be of lower molecular weight than the starting material due to concomitant backbone chain cleavage processes.

The creation of this polar–nonpolar interface leads to interfacial energies that drive phase separation between the two species. Dewetting phenomena have been observed in other systems with AFM techniques.²⁹ The top, higher surface energy species strives to assume spherical morphologies (Figure 2a) to minimize surface area, aided by the increased mobility of the lower molecular weight products.^{17,18} An alternate explanation for the appearance of surface structure is spinodal decomposition, driven by strain release as the initial film undergoes the transition to a new inorganic species. These two mechanisms are currently under consideration in further experiments. Ultimately, the globules and reticulated features become more continuous and increase in height (Figure 2b), leading to the increase in roughness (Table 2).³⁰

In previous literature studies¹ polysilanes such as **2** have been shown to form lithographically imageable in situ hard masks for lithographic image transfer under O₂–RIE conditions, resulting ultimately in a thin coating of etch-resistant SiO_x in the exposed areas. In those studies, various siloxane-containing oligomers and polymers were reported to be formed in the initial etch

stages, leading to softening and perhaps even liquefaction at the surface, with subsequent conversion to a hard SiO_x mask.

Continued oxygen plasma exposure further oxidizes **4**, driving the reaction coordinate in two directions: (i) volatilization of carbon-containing fragments and (ii) immobilization of silicon-containing domains through formation of SiO_x (Scheme 1). This process continues for the silicon-containing polymers until the formation of a contiguous film of SiO_x hardens the surface, restricting surface mobility and protecting the underlying polymer from further oxidation. The continuous SiO_x film is detected in the phase shift channel of the AFM. The lack of contrast in the AFM phase shift image indicates a surface homogeneously coated by a single species.³¹ The chemical composition of the final silicate product is confirmed by Auger and XPS data as being SiO_x.

Support for the proposed reaction scheme is provided by the system's response to changes in the reaction parameters of temperature and atmosphere. Oxygen etching at 0 °C removes carbon-containing moieties and produces SiO_x, yet yields no reticulated morphology—apparently thermal energy is needed to form the reticulation. Furthermore, heating of the starting material **1a** or **1b** alone produces no reticulated morphology when performed in the absence of oxygen. Thus, we conclude that both heating and oxygen are required to produce the final surface pattern in the silicon-containing polymers.

We describe the thermally activated step in the formation of the reticulations in terms of an increase in mobility of the intermediate oxidized fragments **4** of the original silicon-containing polymer **1**. This thermally promoted mobility is enhanced by the decrease in molecular weight of the polymer fragments on etching.

What is the role of the silicon in the RIE of the organosilane polymers? As mentioned earlier, hydrocarbon polymers etch under RIE conditions to the point of complete volatilization. Furthermore, in our study application of the RIE conditions to polymers that contain no silicon results in no reticulated structures. The incorporation of silicon moieties as silicate precursors alters the reaction pathway on etching, or at least introduces additional routes. To better understand the role of silicon in the RIE of organosilanes, several other silicon-containing polymers have been synthesized and

(28) Arkles, B. *Chemtech* **1977**, 7, 766–778.

(29) Overney, R.; et al. *J. Vac. Sci. Technol. B* **1996**, 14, 1276–1279. Overney, R.; et al. *Mater. Res. Soc. Symp. Proc.* **1997**, 464, 133–144.

(30) Reiss, H. *J. Phys. Chem.* **1992**, 96, 4736.

(31) Tamayo, J.; Garcia, R. *Appl. Phys. Lett.* **1997**, 71 (16), 2394–2396.

(32) Greiner, J. H. *J. Appl. Phys.* **1971**, 42, 5151.

subjected to the same reaction conditions as the title disilane polymer **1**.

Polymers **2** and **3**, silicon-backbone polymers with significantly higher molecular weights than **1a** and **1b**, both yield the reticulated geometry of **1** on etching, though on a smaller scale (Figure 4b,c). This is consistent with the silicon being present (1) as a higher percentage of the polymer stoichiometry and (2) in the backbone rather than just in a pendant group. Both of these factors would lead to a more rapid solidification (demobilization) of the SiO_x surface species. The presence of silicon in the starting material also provides a precursor for a *nonvolatile* oxidation product, silicon oxide. This is in contrast to the *volatile* products of carbon oxidation such as aldehydes, alcohols, and acids (vide supra). Polystyrene, a non-silicon-containing polymer, shows no notable surface morphology on etching under our RIE conditions.

Comparison of the etching results for the four polymers (parent disilane, two silicon-backbone polymers, and polystyrene) leads to the conclusion that the role of silicon is critical in producing the reticulated geometry. When the other studied parameters of temperature and atmosphere are taken into account, it is reasonable to conclude that it is the combined processes of oxidation, dewetting, and finally immobilization that lead to the final reticulated surface morphology.

V. Conclusions

We have found that exposing a number of silicon-containing polymers to an oxygen plasma at ambient plasma temperature results in the development of reticulated structures with a size scale on the order of

micrometers. With shorter etch times, a hemispherical/morphology forms which fills out and increases in height with longer etch times.

It was found that by cooling the wafers to 0 °C during reactive ion etching, the reticulated morphology does not develop. We suggest that the formation of surface morphologies requires higher temperatures to facilitate the mobility of silicon-containing polar intermediates as they dewet from the underlying polymer surface to form these reticulated structures.

By XPS and AES, it was found that the silicon in these polymers is converted to SiO_x during oxygen reactive ion etching and that the oxide is localized on the surface.

Acknowledgment. The authors would like to thank Apostolos Avgeropoulos and Nikos Hadjichristidis for the anionically synthesized polymer, Vaughn Deline with his help on Auger electron spectroscopy, George Tyndall with his help on contact angle measurements, and Monika Balk and Martha Harbison for the continuation of this study. The authors would also like to acknowledge CPIMA (Center for Polymer Interface and Macromolecular Assemblies) for partial funding of this research. V.Z.-H.C. would also like to thank the National Science Foundation and IBM for graduate research fellowships.

Supporting Information Available: Text describing FTIR and NMR analyses and figures showing the corresponding spectra for **1a,b** (5 pages). Ordering information is given on any current masthead page.

CM980314+